

Military Technical College
Kobry Elkobbah,
Cairo, Egypt



2nd International Conference
on Electrical Engineering
ICEENG 99

SYSTEMATIC DESIGN PROCEDURE OF SWITCHED RELUCTANCE MOTORS

Amged El-Wakeel* , Said A. Gawish** , M. A. L. Badr***

ABSTRACT

While numerical analysis techniques, such as a finite element analysis and boundary element analysis, have been presented as an accurate tool for design and simulation of Switched Reluctance Motors, they do not give any method of a systematic design procedure with a minimum computational effort. Besides, They have not introduced any matching with the conventional design approaches used in classical machine design. This paper presents a systematic design procedure based on magnetic circuit analysis and standard proportion among motor parts to determine the motor dimensions. The proposed procedure is generally structured to run on personal computers to design and simulate any permissible specifications, in a few minutes. It has been shown that, for fast and more traditional design, no numerical techniques are needed, since the magnetic circuit analysis is more simple and complete in itself. The proposed program is not limited only to the motor iron and copper dimensions, but also estimates many of performance indices such as output power density, generalized power factor, losses and efficiency.

KEYWORDS

Switched Reluctance Motors, Design of Electrical Machines.

NOMENCLATURE

a_w	Wire cross sectional area.	d_{sh}	Shaft diameter.
AR_1	Stator pole aspect ratio.	D	Bore (rotor outer) diameter.
B_s	Saturating flux density.	D_o	Outer motor diameter.
C_o, C_o^1	Normal and maximum Output coefficients.	D_{ri}	Internal diameter of the rotor.
d_s	Stator slot depth.	D_s	Stator airgap diameter.

*** Professor, Dept. Of Elect. Power & Machines, Faculty of engineering, Ain Shams University, Cairo, Egypt. ** Associate professor, Dept. Of Elect. Power & Energy, Egyptian Armed Forces. * M. Sc. , Dept. Of Elect. Power & Energy, Egyptian Armed Forces.

D_{si}	Internal stator diameter.	sr	Split ratio.
E	Motional electromotive force.	t_r, t_s	Rotor and stator pole widths.
f_1	Pole geometry function.	T_a, T_a^1	Average and maximum average torque.
F_1, F_2	Minimum and maximum magneto-motive forces.	V	Applied voltage.
h_{rp}, h_{sp}	Rotor and stator pole heights.	w_{st}, w_{sb}	Top and bottom Slot widths of the stator.
$I_m, I_{r.m.s}$	Maximum and effective phase currents.	W^1	Maximum change of the coenergy.
k_f	Slot filling factor	α	Stator pole arc.
l_g	Airgap length.	β, β^1	Rotor pole and interpolar arcs.
L, L_e	Stack and envelope lengths.	δ	Effective current density.
L_{max}, L_{min}	Maximum and minimum linear self inductance.	θ_s	The mechanical angle of the stator pole pitch.
m	Number of stator poles.	λ_{max}	The maximum aligned flux linkage .
n	Number of rotor poles.	λ_{min}	The minimum unaligned flux linkage .
N_{PH}	Number of turns per phase.	ρ_1, ρ_2	Linear gap permeance functions .
P, P^1	Average and maximum average poweres.	τ_r, τ_s	Rotor and stator pole pitches.

1. INTRODUCTION

Although SRMs are simple in construction they are difficult in design and analysis. These difficulties are summarized mainly in strong spatial and magnetic non-linearities with many flexible design parameters, and interdependence on the design of the converter and control parameters. These difficulties and others accompanied with iron losses and thermal rating prediction make the design procedure of the motor difficult and specialized task.

A variety of publications on the design of SRMs are available and provide a wealthy information regarding the design and construction of SR motors [1:10]. Some of these publications introduce general design considerations and some design equations [1:8] and others demonstrate the applications of computer aided design packages [9,10].

The numerical analysis techniques and integrated design methodology, for SRM have been presented in many publications [11,12]. It has been shown that, for quick and more traditional design, no numerical techniques are required, since the lumped parameter analysis is complete in itself [12,13]. However, for more accurate calculations, numerical techniques can be used to confirm and improve the results of the analytical design work [13].

This paper differs from the previous papers, in the following aspects:

- it presents a systematic routine for the complete motor dimension prediction;

- it requires only one human to computer operation until the solution is found and hence minimum time of execution.
- the proposed program is written in Matlab and is generally structured to run on personal computers to design and simulate any permissible specifications, in a few minutes.

2 DESIGN APPROACH

In this paper, the design is an iterative procedure based on magnetic circuit analysis with approximate flux path calculations which provides fast design of many of the SRM dimensions. Also the design is based on the use of standard proportions and graphical relation among motor parts to determine the rest of dimensions. The static and dynamic simulations of the SRM are included as an integral part of the design procedure in order to predict the motor performance and make design verification.

2.1 Design Limitations

Fig. (1) shows the construction and main dimensions of SRM, and it is clear that a successful design brings out a compromise for space occupied by iron, copper, insulation and air. Actually, the designer must face the general design limitations in choosing the suitable amount and type of materials for the fabrication of the required machine parts. These limitations include the consumer requirements, the saturation level, the allowed temperature rise, the value of power factor, the efficiency and the mechanical design limitations.

The most basic consumer requirements are the output power P_r , the base speed n_r , and the supply voltage V . Temperature rise, envelope dimensions, overload rating, level of protection and maximum noise level are examples of requirements and constraints that may be required [14].

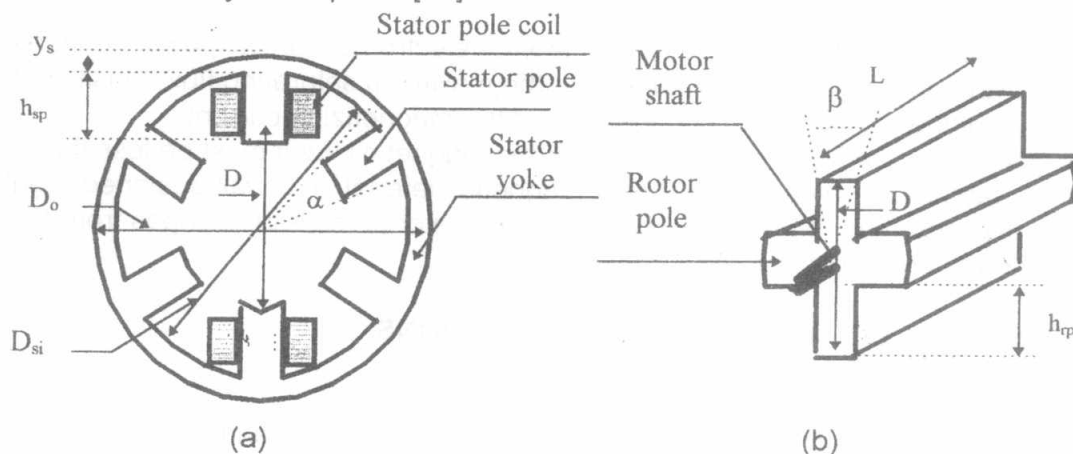


Fig. 1: Motor construction.

(a) Stator dimensions.

(b) Rotor dimensions.

2.3 Design Parameters

Some parameters such as, the number of phases q , number of stator poles m , number of rotor poles n , lamination stacking factor k_{st} and conductor resistivity ρ with its temperature coefficient are usually chosen by the designer and assumed as fixed parameters. Other quasi-fixed parameters like, effective current density δ , saturating flux density B_s are assumed constants with the permeability of minor changes in the iterative design method.

Many parameters such as the outer stator diameter D_o , and airgap length l_g , the stator and rotor pole widths t_s, t_r , and the stator and rotor yoke widths y_s, y_r e.t.c. can be computed from the fixed and quasi-fixed parameters geometrically or by 'ratioing' from the main dimensions, starting from 'standard' proportions.

2.3.1 Choice of Parameters

(i) Choice of the number of phases

From fault tolerance point of view, the fault tolerant motor must be a polyphase motor, and hence all single phase motors are rejected, and from reversible self starting point of view all single and two phase motors are rejected [15].

P. J. Lawrenson [1] explained that, from efficiency point of view, the number of phases must be kept as low as possible to decrease the switching frequency and hence decrease the iron losses. However, if a low speed application is being considered, the limitation imposed by frequency will be less effective and the designer has greater freedom in choice. In practice, the majority of motors have three or four phases, and it is rare to find motors with more than five phases.

(ii) Choice of number of stator and rotor poles

The number of stator poles and rotor poles can be obtained as:

$$m = k q \quad (1)$$

$$n = m - k \quad (2)$$

Where k is an even number. It has been noted that in order to decrease the iron losses and increase the efficiency, the number of poles must be minimum especially in high speed applications, therefore k is usually taken as 2 to decrease the number of stator poles and hence decrease the number of rotor poles [1,5].

(iii) Choice of magnetic loading

The magnetic flux density B is relevant to the electromechanical power conversion process and basically, it is determined by, the maximum saturating flux density in the iron parts of the machine, the iron losses and the magnetizing current.

The maximum flux density in any part of the magnetic circuit must be less than the limiting saturation value of the used magnetic material. In a well-designed regular SRMs the maximum flux density occurs in the stator poles and it ranges from 1.8 to 2.5 Tesla depending on the used material [4].

3 THE OUTPUT EQUATION AND MAIN DIMENSIONS

3.1 Output Equation

The output of a machine can be related to its main dimensions and speed as :

$$P = C_o D^2 L n_r \quad (3)$$

Where C_o is the output coefficient, D is the outer rotor diameter, L is rotor axial length and n_r is the base speed.

References [10] and [16] explained that, it is easy to determine C_o for an existing motor whose power, speed and rotor dimensions are known. For similar cooling, this value is often a convenient starting point for a new design of the same torque, even when the new motor is SRM and the old is conventional.

In this section, The value of C_o will be derived based on the unified approach of static torque production in saturated doubly salient machines [17,18]. As shown in Fig 2, the maximum value of the change in coenergy W^1 (shaded area), as the magneto-motive force F tends to infinity, is equal to the triangular area obc . This yields to:

$$W^1 = \frac{\phi_1^2}{2\mu_o L} \left[\frac{1}{\rho_1} - \frac{1}{\rho_2} \right] \quad (4)$$

Where, ρ_1 and ρ_2 are the linear gap permeance functions in aligned and unaligned positions and the saturation ultimately limits the stator pole flux ϕ to a value ϕ_1 . The average torque T_a can be expressed as [10]:

$$T_a = \frac{q \cdot n}{2\pi} W \quad (5)$$

From equations (1) and (4) into equation (5) the maximum average torque T_a^1 can be expressed as:

$$T_a^1 = \frac{m \cdot n}{4\pi} \cdot \frac{\phi_1^2}{2\mu_o L} \left[\frac{1}{\rho_1} - \frac{1}{\rho_2} \right] \quad (6)$$

The ultimate stator pole flux ϕ_1 can be expressed as:

$$\phi_1 = B_s t_s L k_{st} \quad (7)$$

Where B_s is the peak flux density set by the saturation limit of the stator pole, t_s is the stator pole width and k_{st} is the stacking factor. It is easy seen that the maximum value of the average torque

$$T_a^1 = \frac{\pi \cdot D^2 L k_{st}}{4} \left[\frac{B_s^2}{2 \cdot \mu_o} \right] \left[\frac{t_s^2}{\tau_r \cdot \tau_s} \right] \left[\frac{1}{\rho_1} - \frac{1}{\rho_2} \right] \quad (8)$$

From the previous equation, the maximum average power in KW can be expressed as:

$$P^1 = \frac{\pi^2 10^{-3}}{240 \cdot \mu_o} k_{st} B_s^2 \cdot f_1^1 \cdot D^2 L n_r \quad (9)$$

Where f_1^1 is the maximum value of the gap geometry function f_1 which is given by:

$$f_1 = \left[\frac{t_s^2}{\tau_r \cdot \tau_s} \right] \left[\frac{1}{\rho_1} - \frac{1}{\rho_2} \right] \quad (10)$$

The maximum value of f_1 is about 0.025 which may be used to give a guide to the limiting value of output coefficient predicted by non-linear theory. The result, from equation (10) is:

$$C_o^1 = \frac{\pi}{4} B_s^2 \quad (11)$$

Where C_o^1 ranges from 2.5 to 5 for B_s ranging from 1.75 to 2.5 Tesla.

In an actual machine, the real value of C_o depends on the gap geometry, the saturation level, and the motor mechanical losses. So these effects can be expressed as the correction factor C_r multiplied by the value of C_o^1 .

$$C_o = C_f \frac{\pi}{4} B_s^2 \quad (12)$$

The value of C_f ranges from less than 0.25 for unsaturated small machines and 0.7 for medium saturated machines to 0.98 for high saturated machines with optimum gap geometry which will be explained later.

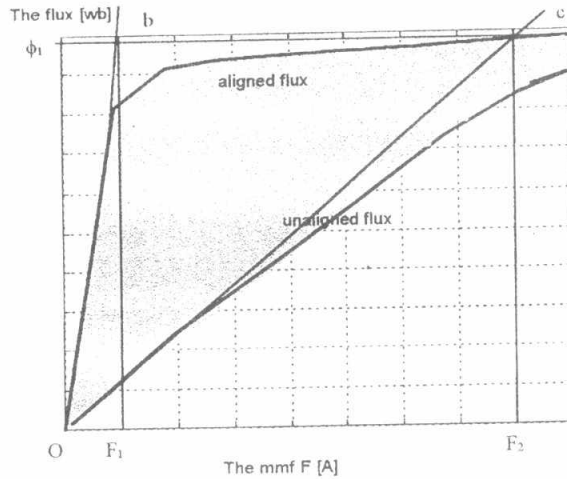


Fig. 2: Stator pole flux against excitation mmf (F).

3.2 Separation of D and L

The factors which influence the relative values of D and L are different for different types of electric machines. For SRM these factors are:

(i) The stator pole proportions

The ratio of core length L to the stator pole pitch τ_s determines the weight of the copper and hence the economics of the machine. This ratio is usually called the stator aspect ratio AR_1 and usually ranges from 1 to 6 for practical SRMs. From this ratio the value of L/D can be computed as:

$$\frac{L}{D} = AR_1 \frac{\pi}{m} \quad (13)$$

For AR_1 ranging from 1 to 6 and m ranging from 6 to 12, the value of L/D ranges from about 0.3 to 3.

(ii) Peripheral speed

Usually, the rotor critical speed imposes a limit on the rotor diameter D [10], because if the rotor peripheral speed V_p is increased, the rotor may be destroyed due to increased centrifugal force.

The peripheral speed may be greater than 175 m/s for high speed SRMs incorporating amorphous iron [17]. However, the peripheral speed usually does not exceed 60 m/s for most normal SRMs.

(iii) Number of poles.

It is advisable to increase the diameter of the machine which has large number of poles. This may be done to obtain sufficient room for the stator coils.

4. STATOR DESIGN EQUATIONS

The stator dimensions include the envelope dimensions, the internal and airgap stator radii and the slot and tooth dimensions. Many of these dimensions can be seen in Fig. 1.a.

4.1 Airgap length and Airgap Stator Diameter

H. C. J. De Jong [20] explained that in the electric machines whose operation is based on permeance fluctuations, the airgap should be as small as mechanically acceptable for obtaining the best electromagnetic performance.

Thus, to maximize the specific torque and minimize the volt-ampere requirements in the controller the airgap length will depend on the mechanical influence only and may be taken as:

$$l_g = 10^{-3} \frac{D}{2} \quad [\text{mm}] \quad , \quad (14)$$

Where, D is the bore diameter measured in [mm]. This relation is restricted with a minimum value of 0.2 mm.

Larger airgap length may be required with special types of bearings, which depend on the machine length. The airgap may be increased to decrease the unbalance magnetic pull, which arises from any small deflection or eccentricity of the rotor shaft.

The following relation may be proposed based on the relation of the airgap length of induction motors and may also be usefully used in SRMs:

$$l_g = 0.2 + 10^{-3} \cdot D \quad (15)$$

The value of l_g usually exists between the two values computed by equations (14) and (15).

The airgap stator diameter D_s can be determined from the motor geometry as:

$$D_s = D + 2 l_g \quad (16)$$

4.2 Envelope Dimensions

The envelope volume may be one of the consumer requirements and in this case the designer must satisfy this restriction in his design.

When the envelope dimensions are not specified, it is easy to estimate them by standard scaling from the main dimensions.

The simplest way to estimate the outer stator diameter D_o is from a typical or standard split ratio sr as:

$$D_o = \frac{D_s}{sr} \quad (17)$$

The value of sr may vary over quite a wide range among 0.4 to 0.7, with most designs around 0.5 to 0.57 depending on the number of stator and rotor poles, and on the operating requirements [14].

The envelope length L_e may be estimated as the stack length plus two end turn overhangs. The overhang length can be approximated as 0.25 of the stator pole pitch, thus, the envelope length can be expressed as:

$$L_e \cong L + \frac{\tau_s}{2} \quad (18)$$

4.3 STATOR TOOTH AND SLOT DIMENSIONS

4.3.1 Tooth Dimensions

Both the stator pole arc α and the corresponding tooth width t_s require careful selection to satisfy the following conditions:

- (i) The stator pole arc must be greater or equal to the step angle to ensure adequate overlap between phases and hence ensure self starting at all rotor positions.
- (ii) The stator pole arc must be less than the rotor interpolar arc β^i to ensure angular clearance between the stator and rotor pole corners and hence ensure sufficiently low unaligned inductance L_u [1,14]. From above conditions α can be expressed as:

$$\alpha_s \leq \alpha \leq \beta^i \quad (19)$$

Where β^i is the rotor interpolar arc and β is the rotor pole arc. Once the stator pole arc has been chosen, the stator pole width can be determined as:

$$t_s = \pi D_s \frac{\alpha}{360} \quad (20)$$

The optimum range for the stator pole arc per stator pole pitch changes according to the objective function. However, in order to optimize the motor performance generally the optimum value can be taken among 0.33 and 0.42 [8].

Stator yoke width y_s is a magnetic relational parameter. So, it can be determined by the solution of the magnetic circuit. The stator pole flux splits equally in both the stator and rotor back irons. Thus the back iron width must support one half of the stator pole flux. If the maximum flux density allowed in the back iron is B_{max} , then the back iron width can be computed as:

$$y_s = \frac{\phi_s}{2 B_{max} k_{st} L} \quad (21)$$

The stator yoke represents the longest path for the magnetic flux, and therefore to decrease saturation and hence decrease the iron losses, we will take the stator back width as 0.55 to 0.75 of the stator pole width t_s [5,8,14].

The stator pole height h_{sp} can be computed as:

$$h_{sp} = 0.5 (D_{si} - D_s) \quad (22)$$

Where D_{si} is the internal stator diameter, D_o is the outer stator diameter and D_s is the airgap stator diameter. This value is exactly true for the trapezoidal pole with a rectangular slot shape.

4.3.2 Slot Dimensions

The slot dimensions are geometrical parameters so they can be computed from the basic stator dimensions. First, the slot depth d_s can be computed as a difference between the internal and airgap stator radii as:

$$d_s = 0.5 (D_{si} - D_s) \quad (23)$$

Second, the slot width at the top of the pole w_{st} , and the slot width at the bottom of the pole w_{sb} can be computed as:

$$w_{st} = D_s \left(\frac{\theta_s - \alpha}{2} \right), \quad (24)$$

$$w_{sb} = D_{si} \left(\frac{\theta_s - \alpha}{2} \right), \quad (25)$$

where, θ_s is the angular stator pole pitch in radians.

5. ROTOR DESIGN EQUATIONS

5.1 Shaft Diameter

For SRM, the weight of the salient structure armature is often less than that of the induction motor, and so, the shaft diameter may be taken as:

$$d_{sh} = \begin{cases} \frac{25 \cdot q}{4} \cdot \sqrt[3]{\frac{P}{n_r}} & \text{for } q \leq 4 \\ 25 \cdot \sqrt[3]{\frac{P}{n_r}} & \text{for } q \geq 5 \end{cases} \quad \text{cm} \quad (26)$$

Although, for high power and high speed applications, the shaft diameter can be taken as that of induction motor.

5.2 Rotor Pole and Yoke Dimensions

The rotor pole arc β and the corresponding tooth width t_r require careful selection to satisfy the following conditions:

(i) The rotor pole arc must be greater or equal to the step angle to ensure self starting of the motor at all rotor positions.

(ii) The rotor pole arc is preferred to be greater than the stator pole arc, this results in a region of constant inductance separating the positive and negative $dL/d\theta$ regions, which in turn provides additional time for the phase current to be completely turned off before the region of negative torque production, i.e.

$$\beta \geq \alpha \quad (27)$$

In terms of widths, t_r should be greater than t_s by about $2l_g$ and the rotor pole width can be computed as:

$$t_r = \pi D \frac{\beta}{360} \quad (28)$$

The rotor yoke width y_r is a magnetic relational parameter which is usually chosen to equalize flux densities in the rotor pole and the rotor yoke irons as:

$$y_r = \frac{t_r}{2} \quad (29)$$

The rotor pole height h_{rp} is a geometrical parameter which can be computed for the trapezoidal pole with a rectangular slot shape as:

$$h_{rp} = 0.5 (D - D_{ri}) \quad (30)$$

where, D_{ri} is the internal rotor diameter.

6 DESIGN OF STATOR WINDING

In SRM, there are two types of coils:

- (i) Dropped in coils, with a maximum slot filling factor of 0.4.
- (ii) Pushed through coils, in which the slot filling factor may be as low as 0.4 for small round conductors increasing to 0.75 for rectangular conductors.

6.1 Number of Turns

In this design approach, the design point is taken to produce the flat topped current waveform at minimum speed at which the full power is produced. According to this approach the back emf E is equal to the dc bus voltage V , the back emf E can be expressed as:

$$E = \omega \frac{\lambda_{\max} - \lambda_{\min}}{\alpha} \quad (31)$$

where λ_{\max} is the maximum aligned flux linkage and λ_{\min} is the minimum or the unaligned flux linkage for the peak phase current.

$$\lambda_{\max} = 0.5 N_{PH} (B_S \cdot k_{ST} \cdot L \cdot D \cdot \alpha) \quad (32)$$

$$\lambda_{\min} = k \lambda_{\max} \quad (33)$$

From equations (31), (32) and (33) the number of turns per phase can be estimated as:

$$N_{PH} = \frac{60V}{(1-k) \cdot K_{ST} \cdot \pi n D L B_S} \quad (34)$$

The value of k depends on the degree of saturation and ranges from less than 0.1 for small unsaturated machines to about 0.5 or more for heavy saturated machines.

6.2 Conductor Area

The conductor area can be computed as:

$$a_w = \frac{I_{R.M.S}}{\delta} \quad (35)$$

Where, $I_{R.M.S}$ is the effective current per phase and δ is the effective current density which ranges from 3 to 6 for totally enclosed natural cooling motors and from 7 to 10 for external self ventilation motors [14].

The effective phase current can be approximated as [6]:

$$I_{R.M.S} = \frac{I_m}{\sqrt{q}} \quad (36)$$

Where, I_m is the maximum flat current which can be computed from Ampere's circuital law at the aligned position. The total copper area per slot must satisfy a filling factor less or equal to the maximum filling factor.

7 DESIGN PROCEDURE RESULTS

In this section the proposed procedure is applied to design a small and fast motor. The main design dimensions and the motor characteristics for 1.1 KW, 6/4, 3-phase, 36 volt, 10000 r.p.m. SRM are summarized in the next table.

Table 1 Main dimensions and characteristics of 1.1 KW, 6/4, 3-phase SRM

Main Parameters	design 1	design 2
Rotor external diameter (D)	0.04 m	0.043 m
Axial length (L)	0.042 m	0.034 m
Internal rotor diameter (D_{ri})	0.027 m	0.028 m
Airgap length (l_g)	0.2 mm	0.2 mm
Stator diameter (D_s)	0.0402 m	0.044 m
Stator internal diameter (D_{si})	0.067 m	0.067 m
Outer diameter (D_o)	0.08 m	0.08 m
Shaft diameter (d_{sh})	0.008 m	0.008 m
Wire cross section area (a_w)	3.464 mm ²	3.464 mm ²
Number of turns (N_{PH})	34 turns	38 turns
Maximum flux density B_s	1.874 Tesla	1.921 Tesla
Maximum phase inductance L_{max}	2.006 mH	2.226 mH
Minimum phase inductance L_{min}	0.181 mH	0.204 mH
Maximum phase current I_m	59.154 A	60.744 A
Ideal Effective phase current I_{eff}	34.133 A	35.071 A
Generalized power factor (PF)	0.613 lag.	0.603 lag.
Copper loss (P_{cu})	0.103 KW	0.108 KW
Mechanical losses (P_{mech})	0.011 KW	0.011 KW
Specific output power	4214.55 KW/m ³	4867.25 KW/m ³
Motor full load efficiency $\eta\%$	84.26 %	83.47 %

From the previous two tables, the increase in the specific output power and hence the decrease in the capital cost leads to a slightly decrease in the efficiency and slightly increase in the running cost. The decrease in efficiency in design 2 is due to the increase in the magnetic and electric loading and hence the increase in the iron and copper losses. The change in ideal dynamic torque curves, linear phase inductance, actual dynamic torque curves and flux linkage are clear from Figures 3 to Fig. 6. In Fig.4, the increase of maximum inductance in design 2 is due to the increase in the number of turns per phase. In Fig.5, negative torques existing in the actual dynamic torque curves will not appear in the shaft and will be canceled with the positive torques of the other phase.

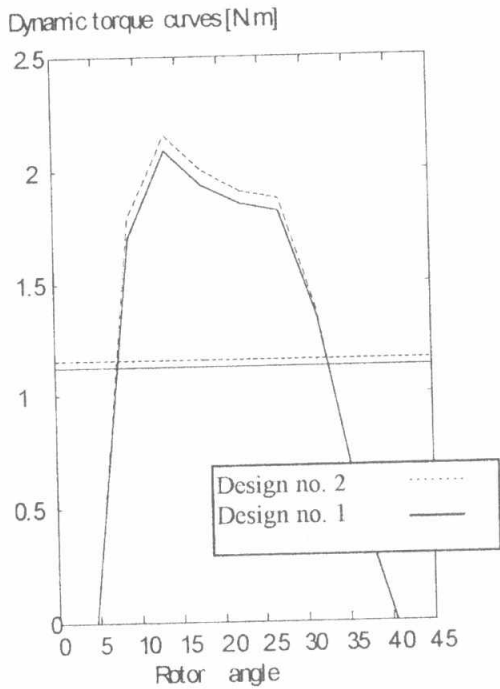


Fig. 3: Per-phase ideal dynamic and average torque curves.

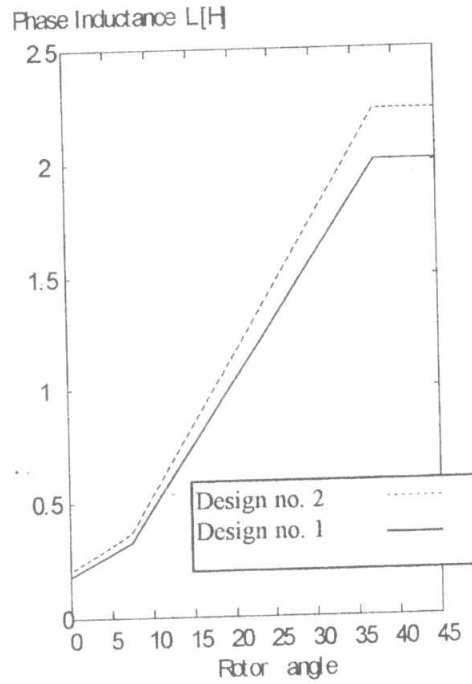


Fig. 4: linear phase inductance.

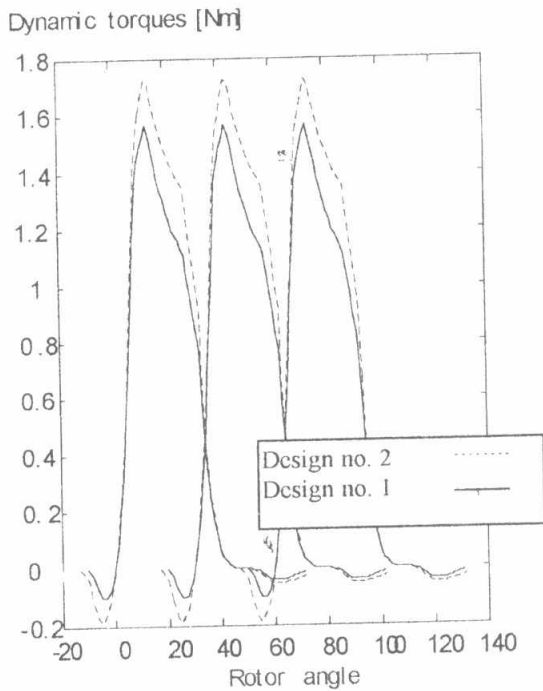


Fig. 5: Actual dynamic torque curves

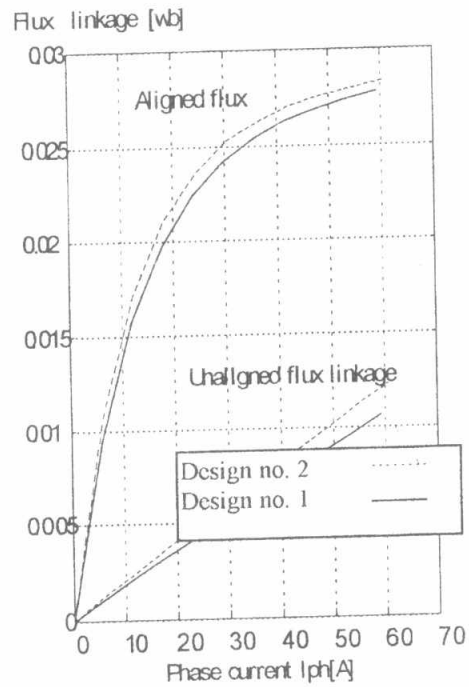


Fig. 6: Aligned and unaligned flux Linkage.

CONCLUSION

The paper introduces a systematic design procedure of SRMs in a manner which is very similar to that used for the traditional machines. This design approach combines magnetic, graphical and relational parameters, in order to estimate the whole motor dimensions. Since, the geometrical parameters and the resulting change in the magnetic flux distribution are related analytically, it is therefore very simple to obtain a basic insight into the effect of various parameters on the magnetic field distribution without the need of many finite element analysis solutions. Finally, the proposed routine makes the design of the motor more popular to designers who are used to the design of conventional machines.

REFERENCES

- [1] P. J. Lawrenson, J. M. Stephenson, J. Corda, and N.N. Fulton, Variable Speed Switched Reluctance Motors. IEE Proc., Vol. 127, Pt. B, No. 4, July (1980), pp. 253 - 265.
- [2] M. Moallem, Chee-Mun Ong, and L. E. Unnewehr, "Effect Of Rotor Profiles on the torque of a Switched Reluctance Motor," IEEE Trans. on Ind. Appl., Vol. IA-28, No. 2, March/ April (1992), pp. 364 - 369.
- [4] Arther V. Radun, "Design Consideration for the Switched Reluctance Motor," IEEE Trans. on Ind. Appl., Vol. IA-31, No. 5, September/ October (1995), pp. 1079 - 1087.
- [5] M. M. Ahmed and M. A. EL-Khazendar, "Optimum Design of an Isolated Switched Reluctance Generator," AL-Azhar Engineering Fourth International Conference December 16 - 19, 1995, pp. 330 - 341.
- [6] J. R. Suriano, and Chee-Mun Ong, "Variable Reluctance Motor Structures For Low Speed Operation," IEEE Trans. on Ind. Appl., Vol. IA-32, No. 2, March/ April 1996, pp. 345 - 353.
- [7] R. Krishnan, R. Arumugam, and J. F. Lindsay, "Design procedure for Switched Reluctance Motor," IEEE Trans. on Ind. Appl., Vol. IA-24, No. 3, May/ June (1988), pp. 456 - 461.
- [8] J. Faiz, and J. W. Finch, "Aspects of Design Optimization For Switched Reluctance Motors," IEEE Trans. on Energy Conversion, Vol. EC-8, No. 4, December (1993), pp. 704 - 713.
- [9] N. N. Fulton, "The Application Of CAD to Switched Reluctance Drives," Electric Machines and Drives Conference, London, UK. December (1987), IEE Conference Publication 282, pp. 275 - 279.
- [10] T. J. E. Miller and M. McGilp, "PC CAD for Switched Reluctance Drives," Electric Machines and Drives Conference, London, UK. December 1987, IEE Conference Publication 282, pp. 360 - 366.
- [11] Yifan Tang and Joseph A. Kline, Modeling and design optimization of Switched reluctance machine by Boundary element analysis and simulation, IEEE Trans. on Energy Conversion, Vol. 11, No.4, Dec. (1996), pp. 673: 680.
- [12] Yifan Tang, Characterization, Numerical Analysis and Design of Switched Reluctance Motors, IEEE Trans. on Ind. Appl., Vol. IA-33, No. 6, Nov. /Dec.(1997), pp. 1544: 1552.
- [13] Duane C. Hanselman, Brushless Permanent Magnet Motor Design, McGraw-Hill, Inc., (1994).

[14] T. J. E. Miller, Switched Reluctance Motors and Their Control. Published jointly by Hillsboro, OH: Magna Physics Tridelta and London, UK: Oxford University Press, (1993).

[15] M. A. L. Badr, R. Mostafa, and A. S. El-Wakeel, "Switched reluctance Drive As Fault Tolerant Drive," Proceeding of the 1st ICEENG conference, M.T.C., Egypt, 24 - 26 March, (1998).

[16] Austin Hughes, Electric Motors and Drives: Fundamentals, Types and Applications, second edition, Newnes, 1994.

[17] K. Backhaus, L. Link, and J. Reinert, "Investigation on a High Speed SRD incorporating Amorphous iron," EPE 95, Sevilla, (1995), pp. 460 - 464.

[18] M. R. Harris, A. Hughes, and P. J. Lawrenson, "Static Torque Production in saturated doubly salient machines," IEE Proc., Vol. 122, No. 10, October (1975), pp. 1121 - 1127.

[19] M. R. Harris, V. Andjagholi, P. J. Lawrenson, A. Hughes, and B. Ertan "Unifying Approach To the Static Torque of Stepping Motor Structures," IEE Proc., Vol. 124, No. 12, December (1977), pp. 1215 - 1224.

[20] H. C. J. DE Jong, A. C. Motor Design With Conventional And Converter Supply. Published by Oxford University Press, 1976, pp. 56 - 58.

[21] A. K. Sawhney, A course In Electrical Machine Design. Dhanpat Rai & Sons, (1982).